JOURNAL OF SOLID STATE CHEMISTRY 8, 57–67 (1973)

Determination of the Homogeneity Range and Refinement of the Crystal Structure of Fe_2P

BERTIL CARLSSON, MARGARETA GÖLIN, AND STIG RUNDQVIST

Institute of Chemistry, University of Uppsala
Box 531, S-751 21 Uppsala 1, Sweden

Received November 27, 1972

The homogeneity range of Fe_2P has been determined using the annealing and quenching technique in combination with X-ray powder diffraction methods. The iron-rich limit is invariant at $Fe_{2.00}P$ for temperatures up to 1150°C. The phosphorus-rich limit varies from $Fe_{2.00}P$ at low temperatures to $Fe_{1.94}P$ at 1100°C. The crystal structure of $Fe_{2.00}P$ has been refined from X-ray diffraction data obtained by single-crystal diffractometry. The thermal vibrations differ appreciably in magnitude for the two non-equivalent types of iron atom.

1. Introduction

The chemical and physical properties of Fe_2P have been the subject of several investigations in recent years (*1–9*). In some instances (*2*, *6*, *7*) measurements have been made on samples, which were stated to contain Fe_2P with a composition deviating from the ideal formula. Although the occurrence of a homogeneity range of Fe_2P was mentioned in the literature as early as 1927 (*10*), no quantitative study of this feature has yet been reported. In the absence of detailed knowledge of the Fe–P equilibrium diagram, the preparation and phase-analytical characterization of Fe_2P samples has remained somewhat uncertain. Accordingly, the results from the property measurements might have a doubtful validity.

In view of these circumstances we have decided to examine some of the properties of Fe_2P more carefully by making an attempt to improve the chemical definition of the test samples. As the basis for this work we have investigated the phase relationships in the solid part of the Fe–P system in the region near $33\frac{1}{3}$ atomic % phosphorus and the results obtained are reported in the present paper. In addition, we present the results from a single crystal structure refinement of Fe_2P.

2. The Homogeneity Range of Fe_2P

2.1. *Previous Work*

The possibility that the compound Fe_2P might have an extended range of homogeneity was first mentioned by Haughton (*10*). He investigated the Fe–P system by classical metallographic methods and presented a constitutional diagram covering the range 0–43 atomic % phosphorus. In the microstructures of alloys with phosphorus contents in excess of $33\frac{1}{3}$ atomic % he observed signs of secondary precipitation of an "unknown constituent" (FeP) in the Fe_2P phase. Accordingly he indicated qualitatively in his equilibrium diagram an extension of the homogeneity range of Fe_2P at higher temperatures towards the phosphorus-rich side. Haughton did not determine the Fe_2P single-phase boundaries quantitatively. His alloys were extremely porous and brittle, which made the preparation of metallographic specimens very difficult.

The compounds Mn_2P, Co_2P and Ni_2P, which are closely related to Fe_2P, have appreciable ranges of homogeneity (*11*, *12*, *13*). The unit cell dimensions of these compounds decrease with decreasing metal content, and particularly large lattice parameter variations have been observed

Printed in Great Britain

(*11*) for Mn_2P. For Fe_2P, however, no lattice parameter variations have been reported.[1] In the present work, preliminary experiments indicated significant variations of the Fe_2P unit cell dimensions in two-phase $Fe_2P + FeP$ alloys quenched from high temperatures. These experiments showed, furthermore, that phosphorus-rich Fe_2P decomposes much more rapidly than Mn_2P, Co_2P and Ni_2P on cooling under similar temperature conditions. The difficulties in retaining phosphorus-rich Fe_2P undecomposed on quenching from high temperatures might explain why changes in the lattice parameters have not been measured in earlier work.

2.2. Experimental Details

On the basis of the preliminary results mentioned above we decided to investigate the homogeneity range of Fe_2P using ordinary X-ray metallographic methods. The normal procedure then is to establish the lattice parameter versus composition relationship from single-phase Fe_2P samples prepared by the annealing and quenching technique. The Fe_2P single phase boundaries are determined by measuring the Fe_2P lattice parameters in two-phase $Fe_2P + Fe_3P$ and $Fe_2P + FeP$ alloys quenched from various temperatures, and using the known relationship between lattice parameters and composition.

TABLE I

POWDER DIFFRACTION DATA FOR Fe_2P^a

I_{obs}	$h\,k\,l$	$\sin^2\theta_{obs}\cdot10^5$	$\sin^2\theta_{calc}\cdot10^5$	d_{calc} (Å)
w	1 0 0	5071	5076	5.081
w^-	0 0 1	10952	10960	3.458
w	1 1 0	15228	15228	2.934
w	1 0 1	16033	16035	2.859
w	2 0 0	20308	20304	2.541
st^+	1 1 1	26189	26187	2.237
st	2 0 1	31262	31263	2.047
st^-	2 1 0	35537	35531	1.921
m^-	0 0 2	43840	43838	1.729
m	3 0 0	45680	45683	1.694
m	2 1 1	46489	46491	1.679

[a] Focusing Hägg–Guinier-type camera (Philips XCD 700), $CrK\alpha_1$ radiation, internal calibration standard germanium ($a = 5.65771$ Å). The data refer to alloy nr 1, $Fe_{2.012}P$ (see Tables II and IV). Weak diffraction lines from Fe_3P present in the powder pattern are not included. Calculated cell dimensions and standard deviations for the Fe_2P phase (24°C): $a = 5.86740(16)$ Å; $c = 3.45809(15)$ Å.

The experimental details of our work are described below.

Powder diffraction patterns were recorded in a focusing Hägg–Guinier-type camera (Philips XCD 700) using monochromatic $CrK\alpha_1$ radiation and zone-refined germanium ($a = 5.65771$ Å at 24°C) as internal calibration standard. The unit cell dimensions were refined by the least squares method using an IBM 1800 computer and the local program CELNE (*14*). The unit cell of Fe_2P is hexagonal (*15*, *16*). Powder diffraction data from a typical measurement are given in Table I.

Iron-phosphorus alloys were prepared as follows. One master alloy, with a nominal composition of about $Fe_{1.8}P$ was synthesized from iron (spectroscopically standardized iron rod, Johnson, Matthey & Co. Ltd.) and red phosphorus (5N, Koch–Light Laboratories Ltd.) by a method differing only in minor details from that described by Haughton (*10*) and Hägg (*15*). The experimental arrangement is shown in Fig. 1. The reaction chamber consists of a silica tube with water-cooled O-ring connectors at both ends. The bottom end is connected to a vacuum pump and the top end is provided with a viewing window, a gas inlet with a manometer, and a horizontal glass tube. The glass tube contains lumps of red phosphorus and a suitably shaped piece of soft magnetic material. Pieces of iron rods are put into a long cylindrical alumina crucible at the centre of the reaction chamber. The chamber is thoroughly evacuated and flushed several times with pure argon and finally filled with argon to a pressure of about 300 torr. The iron is melted by induction heating and, by means of a permanent magnet manipulated from the outside, the phosphorus lumps in the glass tube are successively pushed down through a silica funnel into the melt.

A second master alloy with the approximate composition $Fe_{2.1}P$ was prepared by melting part of the $Fe_{1.8}P$ alloy with pieces of iron in an argon arc furnace. Both master alloys were gently crushed in a Plattner's diamond mortar followed by light grinding in an agate mortar.

Alloys of intermediate compositions were prepared by mixing appropriate portions of the master alloys, heating the mixtures in evacuated and sealed silica tubes and cooling slowly to room temperature.

---

[1] *Note added in proof:* A. Roger (Thesis, University of Paris, 1970) has reported lattice parameter variations for Fe_2P in substantial agreement with our measurements.

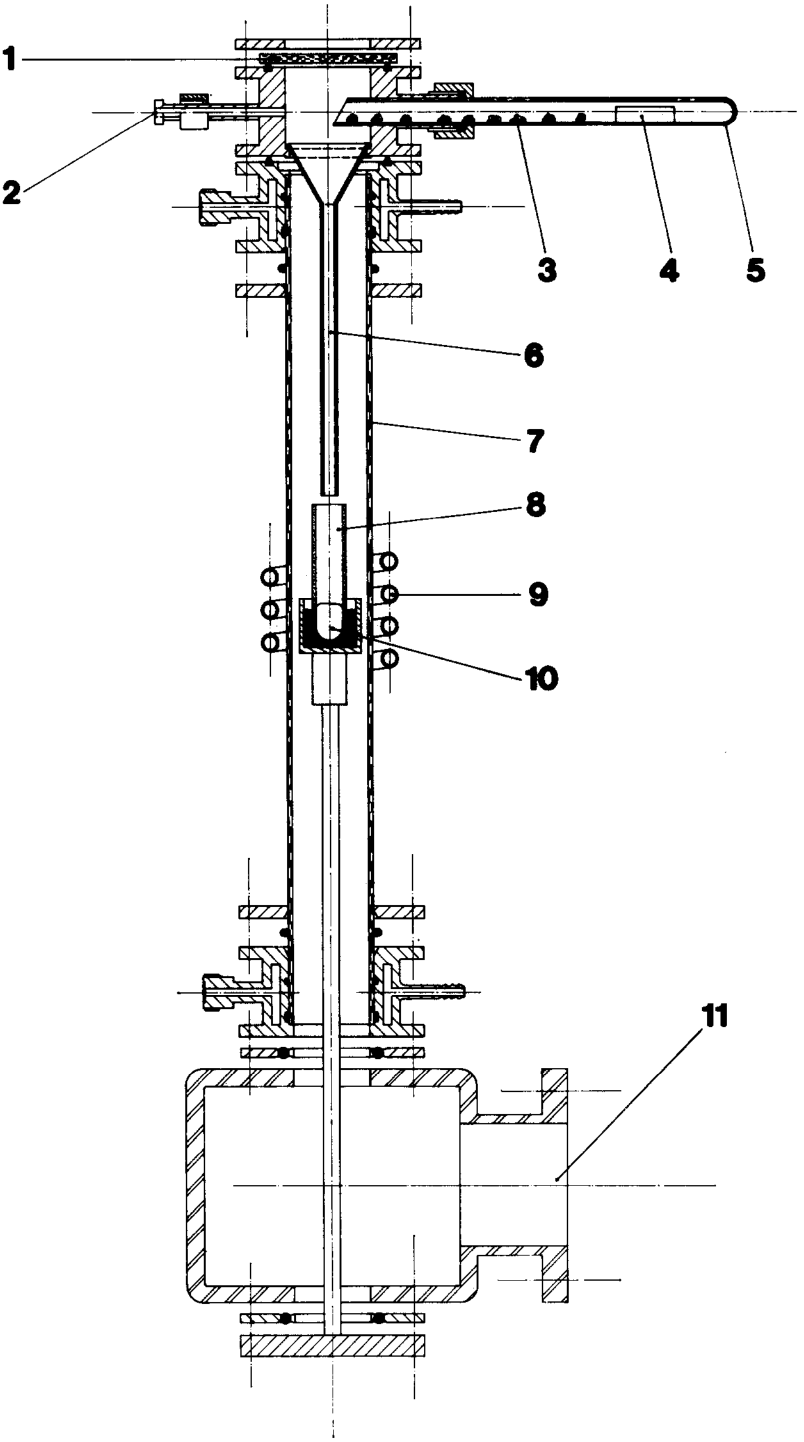

FIG. 1. Induction furnace for phosphide syntheses. (1) viewing window, (2) gas inlet, (3) red phosphorus lumps, (4) soft magnetic iron rod, (5) pyrex glass container, (6) silica funnel, (7) silica tube, (8) alumina crucible, (9) RF work coil, (10) alloy, (11) vacuum connection.

TABLE II

CHEMICAL ANALYSES OF SOME Fe_2P-CONTAINING ALLOYS

Alloy nr	Weight % Fe	Weight % P	Sum	Composition
1	78.36	21.60	99.96	$Fe_{2.012}P$
2	78.30	21.74	100.04	$Fe_{1.998}P$
3	78.24	21.81	100.05	$Fe_{1.990}P$
4	78.02	22.06	100.08	$Fe_{1.962}P$
5	77.80	22.22	100.02	$Fe_{1.942}P$
6	77.56	22.43	99.99	$Fe_{1.918}P$
7	76.74	23.29	100.03	$Fe_{1.827}P$

TABLE III

MASS SPECTROMETRIC DETERMINATION OF IMPURITIES IN Fe_2P-CONTAINING ALLOYS

	Impurities (ppm)					
Alloy	Cu	Sn	Ca	K	Na	W
$Fe_{1.827}P$ (nr 7)	10	—	1.5	—	1.2	<0.6
$Fe_{2.1}P$	31	4	34	21	30	<0.6
$Fe_{1.990}P$ (nr 3)	59	45	20	3.2	6.5	<0.6

The iron and phosphorus content of the alloys was determined by chemical analysis in the following manner. The samples were dissolved in a 1:2 mixture of nitric and hydrochloric acid, and iron and phosphorus were determined in separate aliquots of this solution.

For the determination of phosphorus, hydrochloric acid was removed by evaporation with nitric acid, and the residue was boiled with perchloric acid to complete the oxidation to orthophosphoric acid. Phosphorus was precipitated as ammonium molybdophosphate and weighed as $P_2O_5 \cdot 24\ MoO_3$ according to Nydahl (*17*).

For the determination of iron, nitric acid was removed by evaporation with sulphuric acid. Iron was then reduced by Cr^{2+}, following a procedure developed by Nydahl (*18*), and titrated potentiometrically with cerium sulphate solution, previously standardized against arsenic trioxide (NBS standard).

Analytical results for some alloys of importance in the investigations are given in Table II. The relative errors are estimated to be 0.2% for the phosphorus determination and less than 0.1% for the iron determination.

In order to investigate the impurity content a mass spectrometric analysis was made on selected alloys. The results are collected in Table III. The analyses refer to the two master alloys $Fe_{1.8}P$ (nr 7 in Table II) and $Fe_{2.1}P$ in the as-cast condition, and to alloy nr 3 (Table II) prepared by heating a mixture of the master alloys in a silica ampoule. The arc melting might cause contamination by copper from the hearth and by tungsten from the electrode. For all alloys, the tungsten content was below the limit of detection. The alumina and silica containers are further sources of contamination. Unfortunately, the presence of large amounts of iron prevents the detection of small amounts of aluminium and silicon by the mass spectrometric method.

For practical reasons we decided to perform the annealing treatments of the alloys in evacuated and sealed silica tubes. Special provisions had then to be made in order to ensure sufficiently rapid quenching of the alloys. A simple apparatus was assembled according to Fig. 2 as described below.

The silica ampoule containing the alloy was placed inside a kanthal-wound vertical tube

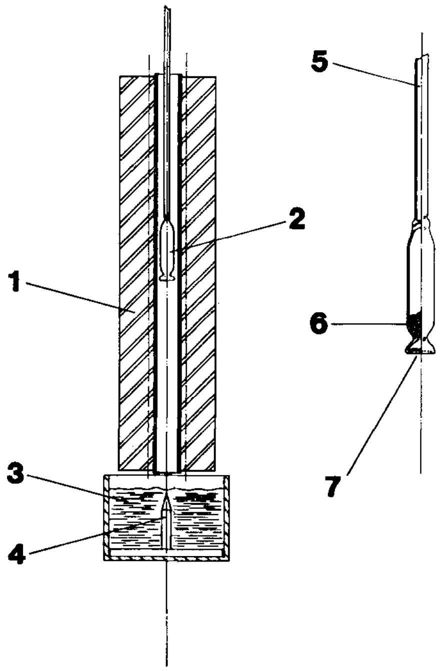

FIG. 2. Device for quenching alloys contained in silica ampoules. (1) kanthal-wound resistance furnace, (2) silica ampoule, (3) cooling medium (brine), (4) steel nail, (5) silica rod, (6) alloy sample, (7) thin-walled concave bottom of ampoule.

furnace equipped with a proportional thyristor controller with PID action (Eurotherm). The temperature was measured with a calibrated Pt–90Pt10Rh thermocouple. It was estimated that the annealing temperatures measured were reliable to within ±2°C. The bottom end of the furnace was placed immediately above a vessel filled with brine. A steel nail fixed on a solid support was placed in the vessel with the hardened tip below the surface of the brine pointing upwards along the axis of the furnace tube.

The silica tube, of a shape as indicated in Fig. 2, was attached to a silica rod extending outside the top end of the furnace. During the annealing treatment both ends of the furnace tube were closed with thermally insulating material. Quenching was performed by pushing the silica rod down to break the bottom of the ampoule against the steel nail. To ensure rapid heat transfer to the cooling medium the alloys were in the form of very thin flakes. It was estimated that the quenching process took less than 0.1 second.

A large number of test runs were made in order to check the annealing and quenching procedure and to get a preliminary outline of the phase boundaries. As judged from the powder diffraction data the alloys reached equilibrium conditions very rapidly at higher temperatures, and an annealing time of one hour was found to be sufficient for temperatures above 750°C.

The efficiency of the quenching process was found to be satisfactory for annealing temperatures up to about 1125°C, provided that the samples were in a finely divided state. For two-phase $Fe_2P + FeP$ alloys quenched from higher temperatures the rate of cooling was insufficient for retaining the Fe_2P phase in a homogeneous condition. The Fe_2P powder diffraction lines were broad, with strongly asymmetric intensity profiles. It appears that a determination of the Fe_2P phase boundaries at temperatures above 1100°C should preferably be made by phase-analytical methods operating directly in the high-temperature region. No efforts were made in the present work to extend the phase boundary determination to temperatures above 1100°C.

For measurements of the lattice parameter versus composition relationship one would normally determine the composition of the Fe_2P phase by chemical analysis of the quenched samples. For obtaining a sufficiently rapid quenching we had to use finely divided material exposing a large surface area to the cooling medium. This introduces a great risk of contaminating the surface layer of the phosphides through reaction with the brine. In fact, we occasionally observed faint extra lines in powder patterns of samples quenched from temperatures about 1100°C, indicating the presence of impurities. In view of these circumstances we felt that chemical analysis of the quenched material would not give very satisfactory results. An alternative procedure would then be to base the conclusions on the compositions of the alloys as analyzed before the final annealing. Accordingly we tried to ascertain that no changes in composition would occur during heat treatments in silica ampoules.

Microscopic examination revealed no signs of attack from the alloys on the silica, and the powder diffraction films showed no lines other than those belonging to the iron phosphides. When the annealing times were extended over more than one day at temperatures over 1000°C, powder diffraction data indicated in a few instances that the phosphides had lost some phosphorus. Phosphorus loss on annealing in silica tubes has been observed previously by Gullman (*19*) in the case of palladium phosphides. The origin of this effect is obscure, but likely explanations might be reaction between the sample and water vapour adsorbed on the silica, or reaction with oxygen diffusing through the walls of the ampoule. In the present study we found that no changes in composition could be detected when a few larger lumps of the alloy were placed together with the thin flakes of material in the ampoule during annealing. The "buffering" action obtained by adding more sample into the ampoules indicates that some reaction involving gaseous components occurs.

For the final measurements, a series of experiments was made, where samples of various compositions were annealed at different temperatures and quenched. The annealing time was restricted to one hour. As indicated by the studies described above, this annealing time should be long enough for attaining equilibrium conditions, but still too short for any appreciable phosphorus losses to occur. The experiments yielded perfectly reproducible and internally consistent data, and the results are presented below.

2.3. Results

The lattice parameter versus composition curves for Fe_2P are shown in Figs. 3a and 3b.

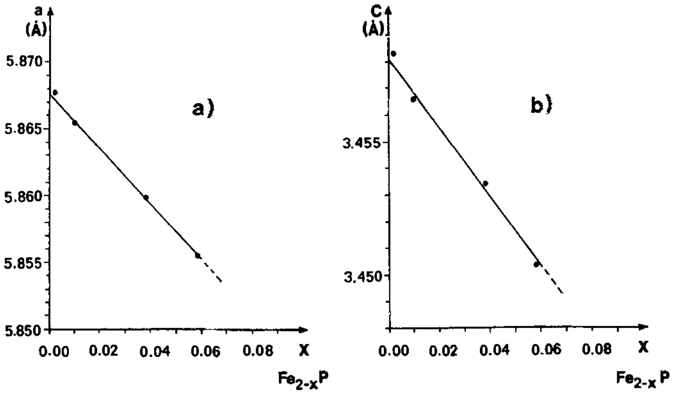

FIG. 3. Lattice parameters of the Fe_2P phase as a function of its composition. (a) variation of the *a* axis, (b) variation of the *c* axis.

The points used for drawing the curves are based on alloys nr 2–5, for which the chemical analyses (before the final annealing) are given in Table II and the annealing temperatures and lattice parameters in Table IV. The powder patterns contained no trace of FeP lines, and the lattice parameters as obtained by quenching from higher temperatures than those quoted in Table IV were unchanged within experimental error.

The limitations of the methods employed are illustrated by alloy nr 6, for which somewhat erratic results were obtained. In one experiment, where the annealing temperature was 1150°C, a powder pattern virtually free from FeP lines was obtained. The profiles of the Fe_2P lines were assymmetric with broad "tails" extending towards the low-angle side. Accordingly, the lattice parameters for this alloy as given in Table IV represent averages for an inhomogeneous material. The results for alloy 6 were therefore neglected when the curves in Fig. 3 were drawn.

The lattice parameters for Fe_2P in two-phase $Fe_2P + Fe_3P$ alloys were found to be constant on quenching from temperatures up to the peritectic temperature for Fe_2P, which is 1166°C according to Haughton (*10*). Within experimental error, the lattice parameters were the same as for alloy 2, $Fe_{1.998}P$. The powder pattern of alloy 2 contained Fe_2P lines only, irrespective of heat treatment. The powder pattern of alloy 1, $Fe_{2.012}P$, contained clearly visible Fe_3P lines in addition to the Fe_2P lines. Alloy 3, $Fe_{1.990}P$, gave in the slowly cooled state a powder pattern with discernible FeP lines, and the cell dimensions of the Fe_2P phase were not very much different from those of alloys 1 and 2. The powder pattern of alloy 3, as quenched from 950°C, showed diffraction lines from Fe_2P

TABLE IV

LATTICE PARAMETERS FOR THE Fe_2P PHASE IN ALLOYS USED FOR ESTABLISHING LATTICE PARAMETER VERSUS COMPOSITION RELATIONSHIP

Alloy nr	Composition	Annealing temp. °C	Phases present	*a* (Å)	*c* (Å)
1	$Fe_{2.012}P$	[a]	$Fe_2P + Fe_3P$	5.8674(2)	3.4581(2)
2	$Fe_{1.998}P$	[a]	Fe_2P	5.8677(3)	3.4584(3)
3	$Fe_{1.990}P$	950	Fe_2P	5.8656(2)	3.4566(2)
4	$Fe_{1.962}P$	1050	Fe_2P	5.8599(2)	3.4534(2)
5	$Fe_{1.942}P$	1125	Fe_2P	5.8555(2)	3.4504(2)
6	$Fe_{1.918}P$	1150	Fe_2P(+FeP)	5.8520(2)	3.4493(2)

[a] Lattice parameters independent of annealing temperature up to 1150°C.

only, and the cell dimensions were significantly smaller than those for the slowly cooled alloy.

From the results quoted above it can be directly concluded that the iron-rich limit of homogeneity for Fe_2P is virtually invariant for all temperatures up to at least 1150°C, and lies between $Fe_{2.012}P$ and $Fe_{1.990}P$. It was obvious by visual inspection of the diffraction films for alloy 1 that the limit of detection for Fe_3P was far from reached. Furthermore, the curves in Fig. 3 indicate that the lattice parameters in alloy 1 correspond very closely to those extrapolated to the ideal composition Fe_2P. It seems safe to conclude that the iron-rich homogeneity limit for Fe_2P lies at $Fe_{2.000\pm0.005}P$ for all temperatures below 1150°C. The results for alloy 3 show that the phosphorus-rich limit at low temperatures is also very near $Fe_{2.00}P$.

Our values for the unit cell dimensions of $Fe_{2.000}P$ (weighted average of several measurements) are: $a = 5.8675(2)$ Å; $c = 3.4581(2)$ Å at 24°C. (Throughout this paper, numbers in parentheses are the estimated standard deviations in the last significant digits).

The phosphorus-rich homogeneity limit was determined using the curves in Fig. 3 and the lattice parameters of the Fe_2P phase as determined in two-phase $Fe_2P + FeP$ alloys quenched from various temperatures. The results are collected in Table V and plotted in Fig. 4. As stressed before, our quenching method could not be used for temperatures above approximately 1125°C.

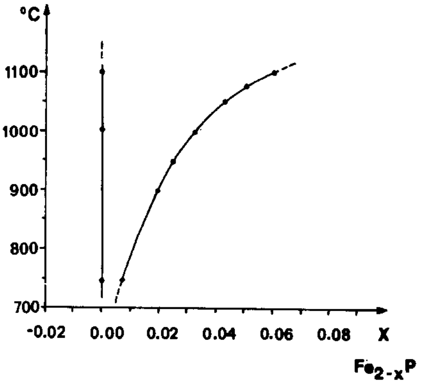

FIG. 4. Single-phase boundaries of $Fe_{2-x}P$ at 750–1100°C.

2.4. *Discussion of the Results*

It is evident from the present results that it is difficult to prepare pure non-stoichiometric Fe_2P samples in sizeable amounts for property measurements at room temperature. The rapid decomposition of phosphorus-rich Fe_2P on passing from the single phase region to the two-phase $Fe_2P + FeP$ region necessitates a very efficient quenching technique. The limiting factor for use of the quenching method is the rate of heat transfer from the sample to the cooling medium. To ensure rapid thermal transport the sample must be in a finely divided state. This means that a large surface area of the material is exposed to chemical attack by the cooling medium, and the purity of the final

TABLE V

LATTICE PARAMETERS FOR THE Fe_2P PHASE IN TWO-PHASE $Fe_2P + FeP$ ALLOYS QUENCHED FROM VARIOUS TEMPERATURES

Alloy nr	Composition	Annealing temp. °C	a (Å)	c (Å)	Composition of Fe_2P phase[b]
3	$Fe_{1.990}P$	[a]	5.8669(2)	3.4579(2)	$Fe_{1.997}P$
7	$Fe_{1.827}P$	750	5.8658(1)	3.4571(1)	$Fe_{1.992}P$
7	$Fe_{1.827}P$	900	5.8636(2)	3.4556(2)	$Fe_{1.980}P$
7	$Fe_{1.827}P$	950	5.8623(2)	3.4548(2)	$Fe_{1.975}P$
7	$Fe_{1.827}P$	1000	5.8608(2)	3.4539(2)	$Fe_{1.967}P$
7	$Fe_{1.827}P$	1050	5.8585(2)	3.4524(2)	$Fe_{1.956}P$
—	$Fe_{1.88}P$	1075	5.8572(1)	3.4514(1)	$Fe_{1.949}P$
—	$Fe_{1.70}P$	1100	5.8550(2)	3.5401(2)	$Fe_{1.939}P$

[a] Slowly cooled.

[b] Composition of Fe_2P phase determined from the curves in Fig. 3.

product might not become very satisfactory. Since quenching from high temperatures has generally not been used for preparing Fe_2P in previous investigations, it appears that most of the measurements reported actually refer to material corresponding closely to the ideal composition $Fe_{2.00}P$. Bellavance et al. (*7*) investigated samples which were stated to consist of single-phase Fe_2P with compositions between $Fe_{2.00}P$ and $Fe_{1.90}P$. Two methods for preparation were used: direct combination of the elements in evacuated silica tubes or high temperature electrolysis of iron- and phosphorus-containing salt baths. In neither case were the samples rapidly quenched from high temperatures. Since the kinetic factors governing the decomposition of phosphorus-rich Fe_2P are not known, the possibility that the nucleation of FeP might be suppressed under certain conditions (as for instance in the electrolytic process) should not be ignored. However, the lattice parameters reported by Bellavance et al. for their various samples are not significantly different from one another, and they agree within experimental error with those obtained for $Fe_{2.00}P$ in the present study. These conclusions have recently been confirmed by Catalano et al. (*27*).

As in the case of Mn_2P, Co_2P and Ni_2P, the cell dimensions for Fe_2P decrease with decreasing metal content. For Co_2P it was shown (*12*) that the deviation from the ideal composition is due to the formation of cobalt vacancies in the crystal structure. There are two crystallographically non-equivalent cobalt positions in the structure, and the crystal structure analysis showed that the vacancies were preferentially distributed on one of these positions. Although Co_2P and Fe_2P are not isostructural, the structures are nevertheless very closely related (*20*), and it is tempting to assume an analogous behaviour of the two compounds with respect to the defects occurring in the structures. The defect structure of Fe_2P will be the subject of further studies to be reported later.

3. Crystal Structure Refinement of Fe_2P

3.1. Previous Work

The first examination of Fe_2P by X-ray diffraction methods was made by Hägg (*15*), who determined the unit cell dimensions and suggested possible hexagonal space group symmetries. Hendricks and Kosting (*21*) made a structure proposal using a trigonal space group. Their proposal was later disproved by Rundqvist and Jellinek (*16*), who derived a structure with hexagonal symmetry in conformity with Hägg's original results. In connection with our work on the physical properties of Fe_2P we found it desirable to possess more accurate crystallographic information, and the present work was therefore undertaken.

3.2. Structure Refinement

A small well-shaped Fe_2P crystal was selected from the $Fe_{2.1}P$ master alloy described in section 2.2. The crystal was in the form of a nearly regular hexagonal prism, bounded by [100] and [001] faces. The height of the prism was approximately 0.08 mm and the average cross-section about 0.05 mm. The powder pattern of the $Fe_{2.1}P$ alloy exhibited perfectly sharp Fe_2P lines, and the cell dimensions agreed within experimental error with those obtained for all other two-phase $Fe_2P + Fe_3P$ alloys. We assumed that the crystal selected for the structure refinement was a representative specimen for the apparently perfectly homogeneous Fe_2P phase in the $Fe_{2.1}P$ alloy. This implies that the compositions of the crystal is very close to the ideal formula Fe_2P and its cell dimensions are $a = 5.8675(2)$ Å, $c = 3.4581(2)$ Å at room temperature (see section 2.3.).

The intensity data were recorded on a Stoe four-circle computer-controlled diffractometer with a graphite monochromator using Mo$K\alpha$ radiation. The intensity measurements were made using the ω–2θ step scan technique. Within the range $0° \leqslant 2\theta \leqslant 100°$, 2458 reflexions were measured corresponding to $-10 \leqslant h \leqslant +10$, $-10 \leqslant k \leqslant +10$ and $0 \leqslant l \leqslant +7$. Three reference reflexions were measured at regular intervals, and these measurements showed that the diffractometer operated in a stable manner during the whole period of data collection. The data were corrected for Lorentz, polarization $[p = (1 + \cos^2 2\theta_M \cos^2 2\theta)/(1 + \cos^2 2\theta_M)$ with $\theta_M = 6.1°]$ and absorption effects using the program DATAPH (*22*) on an IBM 370/155 computer. The calculated linear absorption coefficient was 220 cm^{-1}, and the minimum and maximum transmission factors were 0.333 and 0.430.

An analysis of the corrected intensity data did not indicate any deviation from hexagonal symmetry. Symmetry-equivalent reflexions (twelve recorded equivalents for general reflexions) were then averaged and the number of non-equivalent reflexions thus obtained was 258. The structure was refined by a least-squares procedure using the full-matrix program UPALS (*23*). The structure data given by Rundqvist and Jellinek (*16*) were assumed to be essentially correct and initial parameter values were taken from this source. Atomic scattering factors were taken from (*24*) and dispersion corrections from (*25*). In the first cycles of refinement one scale factor, one positional parameter for each of the two iron positions, and individual isotropic temperature factors for all the non-equivalent atoms were refined. The function minimized was $\Sigma w \cdot (|F_o| - |F_c|)^2$. Weights were assigned to the reflexions according to the formula

$$w^{-1} = \sigma_c^2(F_o) + (0.05\,F_o)^2,$$

where $\sigma(F_o)$ is based on counting statistics. Reflexions with $F_o < 3\sigma_c(F_o)$ were assigned zero weight in the refinements.

At the termination of the refinement the agreement factors were (value for zero-weight data included in parenthesis)

$$R = \Sigma\|F_o|-|F_c\|/\Sigma|F_o| = 0.052\,(0.056)$$

$$R_w = [\Sigma w(|F_o|-|F_c|)^2/w|F_o|^2]^{1/2} = 0.074$$

The isotropic temperature factor for (Fe(1), 0.418(16) Å², was found to be significantly smaller than that for Fe(2), 0.580(17) Å².

In the subsequent refinement, anisotropic thermal parameters and an isotropic extinction parameter, according to the expression by Coppens and Hamilton (*26*) were included. After a few cycles of refinement it was found that the calculated structure factor value for the very strong (002) reflexion remained much larger than the observed value. Zero weight was then assigned to this reflexion and the refinement was continued until all parameter shifts were at least two orders of magnitude less than the calculated standard deviations. The final agreement factors were: $R = 0.032$ (0.037), $R_w = 0.045$. The extinction parameter g (*26*) was 0.065(34), and the extinction correction factor varied between 1.00 and 1.12.

The final structure data obtained are presented in Table VI. Observed (extinction-corrected) and calculated structure factors are listed in Table VII. Interatomic distances are given in Table VIII.

3.3. *Discussion of the Results*

The results of the present structure refinement are in good agreement with those obtained previously (*16*). Since the Fe_2P structure has been thoroughly described and discussed earlier (*16*, *20*) no further comments on the atomic arrangement are given here.

A feature of particular interest is connected with the thermal vibrations in the structure. In a Mössbauer spectroscopic study of Fe_2P (*8*) the room temperature spectrum was resolved into four absorption lines, of which two had a much lower intensity than the remaining pair. The spectrum was tentatively interpreted as follows. Each pair of absorption lines corresponds to one of the two non-equivalent iron positions in the structure. The intensity difference observed is due to a difference in recoil-free fractions for the two types of iron atom. This implies that the thermal vibrations are larger for one of the iron positions than for the other.

TABLE VI

STRUCTURE DATA FOR $Fe_{2.00}P$, INCLUDING ANISOTROPIC THERMAL PARAMETERS β_{ij} ($\cdot 10^4$)[a] AND R.M.S. COMPONENTS R_i OF THERMAL DISPLACEMENTS ($\cdot 10^3$ Å) ALONG THE ELLIPSOID AXES

Atom	Position[b]	x	y	z	β_{11}	β_{22}	β_{33}	R_1	R_2	R_3
Fe(1)	3*f*	0.25683(12)	0	0	34(2)	37(2)	135(4)	66(2)	69(2)	90(2)
Fe(2)	3*g*	0.59461(12)	0	$\frac{1}{2}$	55(2)	76(2)	126(4)	79(2)	100(2)	87(2)
P(1)	2*c*	$\frac{1}{3}$	$\frac{2}{3}$	0	38(2)	β_{11}	127(6)	71(2)	R_1	88(2)
P(2)	1*b*	0	0	$\frac{1}{2}$	50(3)	β_{11}	93(8)	81(3)	R_1	75(3)

[a] The form of the temperature factors is $\exp[-(\beta_{11}h^2 + \ldots + \beta_{12}hk + \ldots)]$.

$$\beta_{12} = \tfrac{1}{2}\beta_{22};\ \beta_{13} = \beta_{23} = 0.$$

[b] Space group $P\bar{6}2m$, $z = 3$; $a = 5.8675(2)$ Å, $c = 3.4581(2)$ Å.

TABLE VII

Observed and Calculated Structure Factors for $Fe_{2.00}P$

		$\lvert F_o \rvert$ ·10	$\lvert F_c \rvert$ ·10	
H,K,0				
1	0	69	62	
2	0	165	149	
3	0	772	707	
4	0	370	347	
5	0	386	376	
6	0	20	16	
7	0	263	257	
8	0	245	243	
9	0	78	80	
10	0	66	66	
1	1	191	168	
2	1	669	649	
3	1	381	351	
4	1	250	233	
5	1	287	278	
6	1	152	149	
7	1	202	196	
8	1	104	103	
9	1	179	176	
10	1	51	42	
2	2	155	133	
3	2	270	256	
4	2	347	333	
5	2	272	259	
6	2	125	121	
7	2	102	100	
8	2	102	97	
9	2	182	184	
3	3	347	355	
4	3	159	154	
5	3	151	150	
6	3	276	284	
7	3	88	89	
8	3	64	64	
9	3	108	113	
4	4	318	307	
5	4	13	8	*
6	4	98	95	
7	4	137	131	
8	4	136	138	
5	5	208	203	
6	5	111	113	
7	5	125	122	
6	6	111	116	
H,K,1				
0	0	112	118	
1	0	113	112	
2	0	684	718	
3	0	66	62	
4	0	315	310	
5	0	368	357	
6	0	47	43	
7	0	97	97	
8	0	65	64	
9	0	59	60	
10	0	190	192	
1	1	835	824	
2	1	300	303	
3	1	342	345	
4	1	213	209	
5	1	295	296	
6	1	278	286	
7	1	173	172	
8	1	148	153	
9	1	140	143	
10	1	89	86	
2	2	227	225	
3	2	526	514	
4	2	182	172	
5	2	244	240	
6	2	191	182	
7	2	221	215	
8	2	91	88	
9	2	38	39	
3	3	54	54	
4	3	111	116	
5	3	103	99	
6	3	41	41	
7	3	190	189	
8	3	103	103	
9	3	38	38	
4	4	394	392	
5	4	46	49	
6	4	86	85	
7	4	182	178	
8	4	96	96	
5	5	235	228	
6	5	102	109	
7	5	71	69	
6	6	11	10	*
H,K,2				
0	0	1117	1277	*
1	0	38	42	
2	0	108	110	
3	0	534	553	
4	0	270	278	
5	0	305	315	
6	0	11	15	*
7	0	228	229	
8	0	218	221	
9	0	68	71	
10	0	65	61	
1	1	121	123	
2	1	453	470	
3	1	273	277	
4	1	197	198	
5	1	235	236	
6	1	127	130	
7	1	175	174	
8	1	95	94	
9	1	163	162	
10	1	42	38	
2	2	119	110	
3	2	203	209	
4	2	278	280	
5	2	229	225	
6	2	108	108	
7	2	90	91	
8	2	91	87	
9	2	167	170	
3	3	280	300	
4	3	134	134	
5	3	131	134	
6	3	247	258	
7	3	81	81	
8	3	61	59	
4	4	272	270	
5	4	13	7	*
6	4	88	86	
7	4	124	119	
5	5	187	184	
6	5	102	103	
7	5	115	114	
6	6	102	107	
H,K,3				
0	0	63	61	
1	0	52	55	
2	0	410	427	
3	0	48	43	
4	0	191	202	
5	0	259	264	
6	0	33	32	
7	0	74	76	
8	0	59	55	
9	0	44	48	
10	0	159	163	
1	1	451	470	
2	1	190	201	
3	1	210	226	
4	1	143	149	
5	1	209	223	
6	1	210	225	
7	1	137	139	
8	1	123	129	
9	1	116	120	
2	2	140	148	
3	2	356	363	
4	2	130	127	
5	2	184	187	
6	2	149	145	
7	2	178	177	
8	2	77	77	
3	3	37	40	
4	3	83	91	
5	3	77	78	
6	3	31	32	
7	3	156	157	
8	3	87	89	
4	4	306	312	
5	4	36	39	
6	4	69	69	
7	4	147	150	
5	5	193	194	
6	5	86	92	
H,K,4				
0	0	629	675	
1	0	29	24	
2	0	64	63	
3	0	325	335	
4	0	168	174	
5	0	206	213	
6	0	16	14	*
7	0	173	172	
8	0	169	171	
9	0	51	51	
1	1	46	49	
2	1	258	267	
3	1	166	169	
4	1	128	130	
5	1	159	162	
6	1	94	94	
7	1	125	126	
8	1	73	74	
2	2	78	71	
3	2	130	134	
4	2	187	190	
5	2	160	157	
6	2	79	80	
7	2	69	69	
8	2	69	65	
3	3	189	206	
4	3	96	97	
5	3	101	101	
6	3	191	200	
7	3	64	65	
4	4	194	194	
5	4	15	6	*
6	4	69	67	
5	5	143	140	
H,K,5				
0	0	34	30	
1	0	25	25	
2	0	237	239	
3	0	23	21	
4	0	125	124	
5	0	163	168	
6	0	33	18	*
7	0	49	50	
8	0	44	43	
1	1	251	255	
2	1	110	116	
3	1	130	138	
4	1	89	90	
5	1	140	146	
6	1	149	156	
7	1	96	97	
2	2	85	89	
3	2	222	224	
4	2	85	81	
5	2	135	132	
6	2	104	100	
3	3	26	23	
4	3	61	64	
5	3	53	51	
6	3	18	20	
4	4	217	216	
5	4	23	27	
H,K,6				
0	0	360	369	
1	0	19	14	*
2	0	43	39	
3	0	191	190	
4	0	112	107	
5	0	140	138	
6	0	26	16	*
1	1	41	35	
2	1	157	154	
3	1	105	103	
4	1	76	72	
5	1	104	103	
2	2	42	36	
3	2	85	83	
4	2	126	122	
5	2	103	98	
3	3	126	131	
4	3	68	65	
H,K,7				
0	0	6	10	*
1	0	29	20	
2	0	137	134	
3	0	10	7	*
1	1	156	148	
2	1	63	62	
3	1	88	87	
2	2	58	55	

Reflexions marked with an asterisk were assigned zero weight in the refinement.

TABLE VIII

Interatomic Distances in $Fe_{2.00}P$ (Å)[a]

Fe(1)–2 P(1)	2.2147(4)	Fe(2)–1 P(2)	2.3787(7)
–2 P(2)	2.2936(5)	–4 P(1)	2.4833(2)
–2 Fe(1)	2.6102(12)	–2 Fe(1)	2.6301(7)
–2 Fe(2)	2.6301(7)	–4 Fe(1)	2.7082(4)
–4 Fe(2)	2.7082(4)	–4 Fe(2)	3.0873(4)
–2 Fe(1)	3.4581(2)	–2 Fe(2)	3.4581(2)
		–1 P(2)	3.4889(7)
P(1)–3 Fe(1)	2.2147(4)	P(2)–6 Fe(1)	2.2936(5)
–6 Fe(2)	2.4833(2)	–3 Fe(2)	2.3787(7)
–3 P(1)	3.3877(1)	–2 P(2)	3.4581(2)
–2 P(1)	3.4581(2)	–3 Fe(2)	3.4889(7)

[a] Distances shorter than 3.7 Å listed.

Thermal vibration parameters for Fe_2P were not available at the time for the Mössbauer study, but structure refinements for the isostructural compounds Mn_2P and Ni_2P (*11*) indicated that the isotropic temperature factors for the Mn(2) and Ni(2) positions were significantly larger than those for Mn(1) and Ni(1). By analogy it was inferred that the thermal vibrations were larger for Fe(2) than for Fe(1), and the low-intensity lines in the room-temperature Mössbauer spectrum were thus ascribed to the Fe(2) atoms. As is evident from the present structure refinement, the thermal vibration parameters for Fe(2) are in fact significantly larger than those for Fe(1), and the previously proposed interpretation of the Fe_2P Mössbauer spectrum is thus supported. A more detailed Mössbauer spectroscopic examination of Fe_2P is currently being made, and the results will be reported later.

Acknowledgments

The chemical analyses of iron and phosphorus were made at the Analytical Department, Institute of Chemistry, Uppsala, by Dr. L. Gustafsson and Prof. F. Nydahl. We are deeply grateful for their excellent work. We are also indebted to Prof. A. Johansson, Royal Institute of Technology, Stockholm, for his work on the mass spectrometric analyses. We would like to thank Mr. H. Karlsson for technical assistance in the diffractometer measurements, Mrs. S. Anugul for valuable aid in evaluating powder diffraction films, and Dr. M. Richardson for correcting the English text of this paper. Financial support from the Swedish Natural Science Research Council is gratefully acknowledged.

References

1. G. Lewis and C. E. Myers, *J. Phys. Chem.* **67**, 1289 (1963).
2. M. C. Cadeville, Thesis, University of Strasbourg, (1966).
3. A. Gérard, *Bull. Soc. Belge Phys.* **1**, 43 (1966).
4. R. E. Bailey and J. F. Duncan, *Inorg. Chem.* **6**, 1444 (1967).
5. K. Sato, K. Adachi, and E. Ando, *J. Phys. Soc. Jap.* **26**, 855 (1969).
6. R. Fruchart, A. Roger, and J. P. Senateur, *J. Appl. Phys.* **40**, 1250 (1969).
7. D. Bellavance, J. Mikkelsen, and A. Wold, *J. Solid State Chem.* **2**, 285 (1970).
8. R. Wäppling, L. Häggström, S. Rundqvist, and E. Karlsson, *J. Solid State Chem.* **3**, 276 (1971).
9. E. Koster and B. G. Turrell, *J. Appl. Phys.* **42**, 1314 (1971).
10. J. L. Haughton, *J. Iron Steel Inst.* **115**, 417 (1927).
11. S. Rundqvist, *Acta Chem. Scand.* **16**, 992 (1962).
12. S. Rundqvist, *Acta Chem. Scand.* **14**, 1961 (1960).
13. E. Larsson, *Arkiv Kemi* **23**, 335 (1965).
14. N. O. Ersson, Institute of Chemistry, Uppsala (1972), unpublished.
15. G. Hägg, *Nova Acta Regiae Soc. Sci. Upsaliensis*, Ser. IV, **7**, No. 1 (1929).
16. S. Rundqvist and F. Jellinek, *Acta Chem. Scand.* **13**, 425 (1959).
17. F. Nydahl, *Lantbrukshögsk. Ann.* **10**, 114 (1942).
18. F. Nydahl, Institute of Chemistry, Uppsala, Technical Note UUIC A (1972).
19. L. O. Gullman, *J. Less-Common Metals* **11**, 157 (1966).
20. S. Rundqvist, *Arkiv Kemi* **20**, 67 (1962).
21. S. B. Hendricks and P. R. Kosting, *Z. Krist.* **74**, 511 (1930).
22. P. Coppens, L. Leiserowitz, and D. Rabinovich, *Acta Cryst.* **18**, 1035 (1965).
23. J.-O. Lundgren, Institute of Chemistry, Uppsala (1972), unpublished.
24. D. T. Cromer and J. T. Waber, *Acta Cryst.* **18**, 104 (1965).
25. D. T. Cromer, *Acta Cryst.* **18**, 17 (1965).
26. P. Coppens and W. C. Hamilton, *Acta Cryst.* **A26**, 71 (1970).
27. A. Catalano, R. J. Arnott, and A. Wold, *J. Solid State Chem.* **7**, 262 (1973).